JACS
JOURNAL OF THE AMERICAN CHEMICAL SOCIETY
Article
pubs.acs.org/JACS

Reactivity of TEMPO toward 16- and 17-Electron Organometallic Reaction Intermediates: A Time-Resolved IR Study

Justin P. Lomont, Son C. Nguyen, and Charles B. Harris*

Department of Chemistry, University of California, Berkeley, Berkeley 94720, California, United States
Chemical Science Division, Lawrence Berkeley National Laboratory, Berkeley 94720, California, United States

Supporting Information

ABSTRACT: The (2,2,6,6-tetramethylpiperidin-1-yl)oxyl radical (TEMPO) has been employed for an extensive range of chemical applications, ranging from organometallic catalysis to serving as a structural probe in biological systems. As a ligand in an organometallic complex, TEMPO can exhibit several distinct coordination modes. Here we use ultrafast time-resolved infrared spectroscopy to study the reactivity of TEMPO toward coordinatively unsaturated 16- and 17-electron organometallic reaction intermediates. TEMPO coordinates to the metal centers of the 16-electron species CpCo(CO) and $Fe(CO)_4$, and to the 17-electron species $CpFe(CO)_2$ and $Mn(CO)_5$, via an associative mechanism with concomitant oxidation of the metal center. In these adducts, TEMPO thus behaves as an anionic ligand, characterized by a pyramidal geometry about the nitrogen center. Density functional theory calculations are used to facilitate interpretation of the spectra and to further explore the structures of the TEMPO adducts. To our knowledge, this study represents the first direct characterization of the mechanism of the reaction of TEMPO with coordinatively unsaturated organometallic complexes, providing valuable insight into its reactions with commonly encountered reaction intermediates. The similar reactivity of TEMPO toward each of the species studied suggests that these results can be considered representative of TEMPO's reactivity toward all low-valent transition metal complexes.

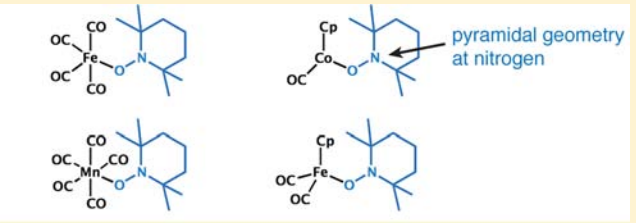

1. INTRODUCTION

(2,2,6,6-Tetramethylpiperidin-1-yl)oxyl (TEMPO) is a stable nitroxyl radical with a remarkably broad range of applications in chemistry, including numerous examples in the field of organometallic catalysis. TEMPO is a popular reagent for the oxidation of alcohols,[1] and TEMPO-based catalysts have been employed for various industrial applications, often with environmental and health benefits over alternative methods.[2] Further applications of TEMPO include catalysis of the Pauson-Khand reaction,[3] oxidative couplings of arenes,[4] nitration of olefins,[5] and the synthesis of monodisperse cobalt oxide nanoparticles.[6] TEMPO is also commonly used as a radical trap and polymerization reagent[7] and as a structural probe of biological systems via EPR measurements.[8]

The behavior of TEMPO as a ligand is a topic of significant interest, as its bonding and reactivity carry mechanistic implications for the myriad of chemical processes mentioned above. Literature reports have established three distinct modes of coordination of TEMPO to individual metal centers (see Figure 1), as well as additional examples involving TEMPO as a bridging ligand between pairs of metal centers,[9] demonstrating that its behavior as a ligand is as varied as its chemical applications. In the present study, we use picosecond time-resolved infrared (TRIR) spectroscopy to directly characterize the reactivity of TEMPO as a ligand toward coordinatively unsaturated 16-electron (16e) and 17-electron (17e) organometallic photoproducts, which are representative of commonly encountered intermediates in organometallic reaction mechanisms. Our observations make use of the structurally sensitive CO-stretching frequencies of the metal−carbonyl photoproducts to monitor the reaction with TEMPO.

Figure 1. Representative examples of coordination geometries for TEMPO adducts (refs 9−17).

TEMPO may coordinate to individual metal centers with either η^1 or η^2 hapticity, with two possibilities for the electronic structure of the η^1-coordinated TEMPO ligand. η^1 TEMPO ligands may either effectively undergo an internal oxidation/reduction process with the metal center, resulting in an anionic TEMPO ligand, or they may behave as radical 1e donors, with no oxidation/reduction taking place.[9−13] This distinction is more than a mere issue of electron counting, as the two

Received: May 5, 2013
Published: July 2, 2013

   dx.doi.org/10.1021/ja404476m | J. Am. Chem. Soc. 2013, 135, 11266−11273

situations result in clearly distinguishable bonding geometries at the nitroxyl nitrogen atom; anionic TEMPO ligands are characterized by a nitrogen atom that adopts a pyramidal geometry, while the radical TEMPO ligand maintains a planar geometry about the nitrogen center. These differences have been established by characterization of the crystal structures of various TEMPO adducts involving metals including Li, Na, Mg,[9] Ti,[10] Ga,[11] Pd,[12] Cu,[13] Fe,[14] and Al.[11,14] Examples of η^2-coordinated TEMPO adducts include the 16-electron (16e) complexes (TEMPO)$Co(CO)_2$ and (TEMPO)$Mn(CO)_3$, or the 14-electron (14e) complex (TEMPO)$V(CO)_3$, which are formed via reactions with $Co_2(CO)_8$,[15] $Mn_2(CO)_{10}$,[16] or $V(CO)_6$ (a 17e complex),[17] respectively. The reactions with metal carbonyl dimers presumably proceed via homolysis of the metal−metal bond.

While the mechanisms of TEMPO-catalyzed oxidation reactions have been studied by several authors,[18] the coordination chemistry of TEMPO has been much less thoroughly investigated, and many key reaction intermediates have never been directly observed. There remains substantial debate in the literature regarding the mechanism of alcohol oxidations.[13,14,19−23] At present, there exist no clear rules for predicting the nature of coordination of a TEMPO ligand in a given complex. In this study, we use ultrafast TRIR spectroscopy to directly characterize the adducts formed following the reaction of TEMPO with coordinatively unsaturated 16e and 17e metal carbonyl reaction intermediates in solution. Density functional theory calculations are used to facilitate interpretation of the experimental results. Metal carbonyl complexes represent one of the most widely used classes of organometallic reagents and catalysts, and thus the reactivity of TEMPO toward these species is broadly relevant to chemists working with this increasingly popular, coordinatively versatile reagent. For each of the 16e and 17e intermediates studied, TEMPO coordination is observed to take place with concomitant oxidation of the metal center, yielding adducts containing anionic TEMPO ligands. No other ligand substitutions or distortions are observed. The similar reactivity of TEMPO with each of the intermediates studied suggests that these observations are representative of TEMPO's reactivity toward low-valent transition metal complexes in general.

2. METHODS

2.1. Sample Preparation. $CpCo(CO)_2$, $Fe(CO)_5$, $[CpFe(CO)_2]_2$, $Mn_2(CO)_{10}$, (2,2,6,6-tetramethylpiperidin-1-yl)oxyl (TEMPO), and cyclohexane were purchased from Sigma-Aldrich Co. All samples and solvents were used without further purification. Dilute solutions of all samples were stable in air at ambient temperatures for at least a few hours (verified via FTIR).

B. Ultrafast UV/Visible Pump−IR Probe Spectroscopy. The experimental setup consists of a Ti:sapphire regenerative amplifier (SpectraPhysics, Spitfire) seeded by a Ti:sapphire oscillator (SpectraPhysics, Tsunami) to produce a 1 kHz train of 100 fs pulses centered at 800 nm with an average pulse power of 1.1 mJ. The output of this commercial system is split, and 30% of the output is used to generate 400 and 267 nm pump pulses (80 and 6 μJ per pulse at the sample, respectively) via second and third harmonic generation. The other 70% is used to pump a home-built two-pass BBO-based optical parametric amplifier (OPA),[24] the output of which is mixed in a $AgGaS_2$ crystal to produce mid-IR probe pulses tunable from 3.0 to 6.0 μm with a 200 cm^{-1} spectral width and a ∼100 fs pulse duration. The 400 and 267 nm pulses pass through a 25 cm silica rod, which stretches the pulses in time to 1 ps, and gives a cross correlation of the mid-IR and 400 or 267 nm pulses of 1.1 ps at the sample. The stretched 400 and 267 nm pulses are necessary to achieve high pump powers without generating products resulting from multiphoton excitation. The stretched pulses also reduce artifacts resulting from nonlinear optical effects in the sample cell windows.

The polarization of the pump beam is held at the magic angle (54.7°) with respect to the mid-IR probe beam to eliminate effects from rotational diffusion. A computer-controlled translation stage (Newport) allows for variable time delays up to ∼1.5 ns between pump and probe pulses. The sample is flowed using a mechanical pump through a stainless steel cell (Harrick Scientific) fitted with 2 mm thick CaF_2 windows separated by 100, 150, or 250 μm spacers. The pump and probe beams are spatially overlapped at the sample and focused so that the respective beam diameters are ∼200 and 100 μm. The sample cell is moved by computer-controlled translational stages (Standa) during the course of data collection so that absorptions are not altered by any accumulation of photoproduct on the sample windows. Reference and signal mid-IR beams are sent along a parallel path through a computer-controlled spectrograph with entrance slits set at 70 μm (Acton Research Corporation, SpectraPro-150) and detected by a 2 × 32 element MCT-array IR detector (InfraRed Associates, Inc.) and a high-speed signal acquisition system and data-acquisition software (Infrared Systems Development Corp.) with a resolution of ∼2.5 cm^{-1}. Collected signals are averaged over 2×10^4 laser shots to correct for shot-to-shot fluctuations. Differences in optical density as small as 5×10^{-5} are observable after 1 s of data collection.

2.3. Data Analysis. Kinetic data in this work result from spectra measured at delay times between 0 and 1000 ps between the visible-pump and IR-probe pulses. Kinetic traces for each spectral feature were obtained by integrating a narrow spectral region (∼5 cm^{-1} wide) surrounding the reported frequency. The kinetic data were then fit to exponential curves using Origin Pro 8 software.[25] Errors on experimental time constants are reported as 95% confidence intervals.

2.4. DFT Modeling. Density functional theory (DFT) calculations have been carried out to facilitate assignment of the absorptions observed in the TRIR spectra. Calculations were carried out using the BP86,[26] B3LYP,[26a,27] M06,[28] PBE0,[29] PW91,[30] and WB97[31] functionals in the *Gaussian09*[32] package using the 6-311+g(d,p) basis[33] for all atoms. Geometry optimizations were followed by a frequency analysis for use in interpreting the TRIR results and to ensure that all geometries are genuine local minima. As DFT methods are known to have difficulty accurately predicting bond enthalpies for TEMPO and other radicals, we use only the calculated frequencies in interpreting the experimental observations.[34]

3. RESULTS AND DISCUSSION

TRIR spectra in the CO-stretching region are presented as difference absorbance spectra. Positive absorptions correspond to newly formed species, while negative bands correspond to the depletion of parent molecules. Data were collected using 400 nm excitation, as initial experiments indicated that the relative absorption cross sections of TEMPO and the metal carbonyl species, combined with the weaker 267 nm pump power, rendered collection of quality TRIR spectra at the 267 nm excitation wavelength infeasible (see SI for the UV−vis spectrum of TEMPO in cyclohexane solution).

3.1. Ultrafast Reactivity of TEMPO toward 16-Electron Photoproducts. Beginning from a stable 18e organometallic complex, thermal or photochemical dissociation of a 2e ligand leads to the formation of a relatively reactive 16e species. In this study, we have characterized the reactivity of the TEMPO radical toward the 16e $CpCo(CO)$ and $Fe(CO)_4$ photoproducts, which serve as representative examples of 16e intermediates in organometallic reaction mechanisms. The literature contains ample reports on the reactivity of these prototypical 16e photoproducts, which facilitates interpretation of the experimental results in cyclohexane/TEMPO solution. Spectra were collected at varied TEMPO concentrations; the

spectra collected at lower TEMPO concentrations generally yielded better signal-to-noise, and here we present spectra collected at concentrations that allow clear visualization of the conversion of each photoproduct to the corresponding TEMPO adduct, while maintaining quality signal-to-noise ratios.

3.1.1. Reactivity of TEMPO toward CpCo(CO). In alkane solution, 400 nm photolysis of $CpCo(CO)_2$ leads to formation of $^3CpCo(CO)$, characterized by its absorption band at 1989 cm^{-1}, along with excitation into an electronically excited state of the parent molecule that relaxes completely within the first 100 ps. Figure 2 shows TRIR spectra of $CpCo(CO)_2$ collected

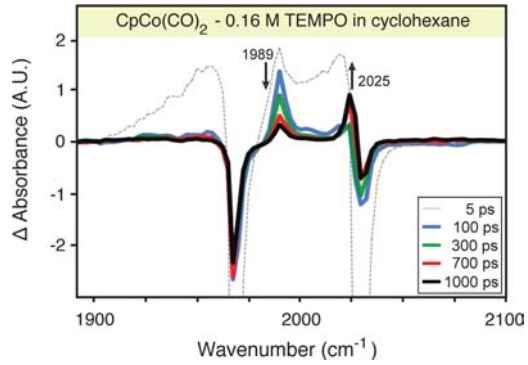

Figure 2. TRIR spectra of $CpCo(CO)_2$ in 0.16 M TEMPO/cyclohexane solution following 400 nm photolysis.

following 400 nm excitation in a 0.16 M solution of TEMPO in cyclohexane solvent. At early delay times (see 5 ps spectrum), the positive features in the spectra are dominated by broad absorption bands due to the electronically excited parent complex. The negative bleaches at 1967 and 2029 cm^{-1} correspond to depletion of the parent $CpCo(CO)_2$ complex. The band at 1989 cm^{-1}, corresponding to $^3CpCo(CO)$, decays with a time constant of 274 ± 32 ps (k_{bimol} = 2.3 × 10^{10} M^{-1} s^{-1}),[35] with the concomitant rise of a new band at 2025 cm^{-1}, attributed to the TEMPO adduct. Data collected at higher TEMPO concentrations (e.g., 0.32 M TEMPO) shows complete conversion of $^3CpCo(CO)$ at a 1 ns delay time.

It is noteworthy that this new CO absorption band is at a higher frequency than that of $^3CpCo(CO)$; coordination of a solvent molecule as a token ligand to CpCo(CO) typically results in a decreased CO-stretching frequency for the lone carbonyl ligand, presumably due to increased π-backbonding from the Co center.[36,37] In the spectra shown in Figure 2, we interpret the increase in CO-stretching frequency to suggest a decrease in π-backbonding to the CO ligand upon coordination of the TEMPO ligand, suggesting a decrease in electron density at the Co center.

As was mentioned in the introduction, TEMPO can coordinate to a single metal center with either η^1 or η^2 hapticity, with either an anionic or radical electronic configuration in the η^1 geometry. To coordinate to 16e CpCo(CO) with an η^2 geometry and not exceed an 18e count at the metal center, either the carbonyl ligand would have to dissociate, or the Cp ring would have to distort. Considering that the observed TEMPO adduct clearly contains a CO ligand, and that the observation of a stable ring-slipped product in the solution phase would be exceedingly rare,[38] we conclude an η^1 coordination geometry for TEMPO. Of the two possibilities for η^1 coordination, only the anionic coordination mode would be expected to reflect an oxidation of the metal center, consistent with the relatively high frequency of the IR absorption band observed for the CpCo(CO)(TEMPO) adduct. This strongly suggests that the TRIR results indicate an anionic TEMPO ligand. Density functional theory (DFT) calculations were carried out to further investigate the structure of this adduct.

Geometry optimizations and frequency calculations were carried out using six DFT functionals (see Table 1), including

Table 1. Experimental and Calculated Frequency Shifts upon Coordination of TEMPO (nitroxyl group) to $^3CpCo(CO)$[a]

functional	$\Delta\upsilon_{TEMPO}$[b] (cm^{-1})	$\Delta\upsilon_{Butanol,singlet}$[b] ($cm^{-1}$)	$\Delta\upsilon_{Butanol,triplet}$[b] ($cm^{-1}$)
B3LYP	22	−59	−35
BP86	5	−43	−36
M06	23	−56	−36
PBE0	48	−56	−37
PW91	5	−43	−37
WB97	36	−66	−42
experiment:	36	−73	−42

[a]Previous results for coordination of 1-butanol from ref 37c are provided for comparison. [b]Calculated frequency shifts are reported relative to the CO-stretching frequency calculated for $^3CpCo(CO)$. No scaling factors were used.

both hybrid and pure density functionals. Previous investigations into the ability of various DFT functionals to accurately predict the difference in energy between the singlet and triplet states for 16e CpCo(CO) have demonstrated that pure density functionals (e.g., BP86 or PW91) are better able to predict this energy gap.[37,39] Upon coordination of the doublet TEMPO ligand to $^3CpCo(CO)$, our results suggest that a doublet ground state is favored by 8−20 kcal/mol, relative to a quartet.

Geometry optimizations indicate that TEMPO coordinates to the metal center in an η^1 fashion (see Figure 3), consistent

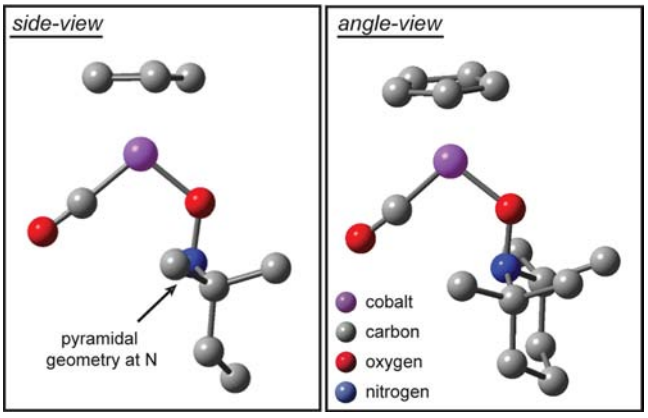

Figure 3. DFT (B3LYP) calculated structure for the CpCo(CO)-(TEMPO) adduct (H-atoms omitted for clarity).

with our aforementioned reasoning. As discussed in the introduction, previous work has established that anionic TEMPO ligands are characterized by a pyramidal geometry at the nitroxyl nitrogen, while a radical TEMPO ligand maintains a planar geometry at the nitrogen center. With each functional tested, the nitrogen atom of the CpCo(CO)(TEMPO) adduct clearly adopts a pyramidal geometry, indicating the presence of an anionic TEMPO ligand. The sum of the bond angles about

dx.doi.org/10.1021/ja404476m | J. Am. Chem. Soc. 2013, 135, 11266−11273

the nitrogen atom is 336.1° (B3LYP value). For comparison, calculations on the free (non-coordinated) TEMPO ligand were also carried out, and each functional also correctly predicts a nearly planar geometry for the free TEMPO radical. Reduction of the TEMPO ligand, and thus oxidation of the Co center, is consistent with the experimentally observed blue-shift in the CO-stretching frequency upon TEMPO coordination; whereas coordination of most 2e donor ligands results in a decrease in the experimentally observed CO-stretching frequency, the fact that coordination of TEMPO results in an increase in the CO-stretching frequency suggests decreased π-backbonding from the Co center to the CO ligand.

Indeed, the calculated CO-stretching frequencies predict an increase in CO-stretching frequency upon coordination of TEMPO (Table 1). For comparison, the analogous experimental and calculated values are also shown for both the singlet and triplet 1-butanol-coordinated adducts observed in a previous study;[37c] these are provided to demonstrate the ability of DFT calculations to reproduce experimentally observed changes in CO-stretching frequencies. While these calculated frequency shifts are not expected to be quantitatively accurate, it is striking that the changes in experimentally observed CO-stretching frequencies upon coordination to TEMPO and 1-butanol are qualitatively well-reproduced by the DFT calculations. These calculated frequencies, in conjunction with the experimental results and calculated geometries, support assignment of TEMPO in the CpCo(CO)(TEMPO) adduct as an anionic TEMPO ligand (refer to Figure 1), effectively resulting in a Co(II) complex. As was mentioned earlier, the simple fact that the experimental CO-stretching frequency increases upon coordination of TEMPO provides strong, stand-alone evidence that TEMPO has oxidized the metal center. The good agreement between calculation and experiment in this spectroscopically straightforward adduct (i.e., containing a single CO oscillator) supports the notion that DFT methods are useful for predicting the behavior of TEMPO as it reacts with coordinatively unsaturated organometallic intermediates.

3.1.2. Reactivity of TEMPO toward Fe(CO)$_4$. Photolysis of $Fe(CO)_5$ at 400 nm in cyclohexane solution leads to formation of $^3Fe(CO)_4$, characterized by absorption bands at 1965 and 1987 cm^{-1}, along with a small amount of $^1Fe(CO)_4$(cyclohexane), characterized by absorption bands at 1950, 1970, and 1986 cm^{-1}.[40] TRIR spectra of $Fe(CO)_5$ collected following 400 nm excitation in a 0.32 M solution of TEMPO in cyclohexane solvent are shown in Figure 4. A higher concentration of TEMPO was used in this case so that the conversion of photoproducts to TEMPO-coordinated adducts could be observed more clearly on the picosecond time scale. Bands at 1965 and 1987 cm^{-1} decay with increasing decay time, accompanied by the growth of new bands at ~1985 and 2041 cm^{-1}, attributed to formation of an Fe(CO)$_4$(TEMPO) adduct; note that the band at 1987 cm^{-1} appears to shift as it decreases in intensity due to its overlap with the band of the TEMPO adduct at at 1985 cm^{-1}. The relatively static absorption band at 1949 cm^{-1} is attributed to $^1Fe(CO)_4$(cyclohexane). At a 0.32 M concentration of TEMPO, the rise time of the band at 2041 cm^{-1} is 634 ± 102 ps (k_{bimol} = 4.9 × 10^9 M^{-1} s^{-1}). On the basis of comparisons to previous time-resolved studies on $Fe(CO)_4$ photoproducts,[40] the TEMPO adduct may also be found to have a weak absorption band near 1965 cm^{-1} overlapping that of $^3Fe(CO)_4$. Multiple CO-dissocaition processes can be ruled out, as the incident photon energy at 400 nm is too weak to lead directly to multiple CO-loss in the solution phase; also, previous studies have examined the spectra of ligand-induced multiple CO-loss for this photoproduct, and the presence of the band at 2041 cm^{-1} is inconsistent with such a process.[37a]

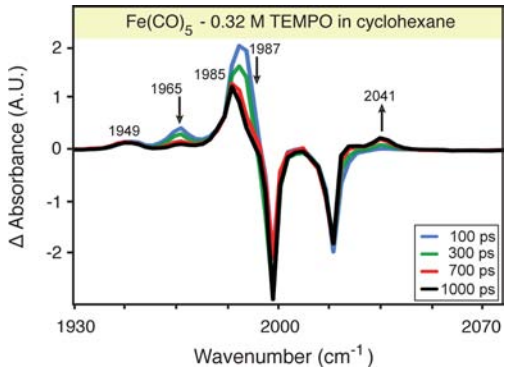

Figure 4. TRIR spectra of $Fe(CO)_5$ in 0.32 M TEMPO/cyclohexane solution following 400 nm photolysis.

Changes in geometry and the coupling of local modes upon TEMPO coordination make it less straightforward to assign an oxidation state to the TEMPO ligand based purely on the experimental data than in the case of the CpCo(CO)(TEMPO) adduct. However, it is useful to compare the present spectra to those observed in a previous solution phase study on $Fe(CO)_4$ adducts formed with the 2e donor PEt_3, or with alcohol solvents.[37a] For $Fe(CO)_4PEt_3$, the major CO-stretching absorptions are located at 1932 and 2047 cm^{-1}, and for $Fe(CO)_4$(alcohol) these are located at 1950 and 2047 cm^{-1}. In each case, the lower frequency bands most likely correspond to an overlapping combination of the B_1 and B_2 bands, with the higher frequency band assigned to an A_1 mode. The notably higher frequency of the B_1/B_2 band (1985 cm^{-1}) in the TEMPO adduct may suggest that the Fe center is less able to effectively π-backbond, though the similar frequencies of the A_1 modes in all three cases are not as conclusive. For this reason, DFT geometry optimizations and frequency calculations were also used to study the oxidation state of the TEMPO ligand in this adduct.

Using each of the six functionals tested, the DFT calculated geometries show a pyramidal coordination geometry about the nitrogen center (sum of bond angles equal to 334.1° with B3LYP), indicating that TEMPO is reduced to an anionic ligand. To check for consistency with the experimentally observed IR spectra, frequency calculations were carried out. We have used the calculated frequency gap between the highest-frequency CO-stretching (A_1) mode and the next highest frequency (B_1) mode to compare with the splitting between the experimentally observed bands (Table 2). As is evident from the values in Table 2, these calculated frequency gaps are consistent with the gap observed experimentally, supporting assignment of the experimentally observed TEMPO adduct to anionic TEMPO ligand adduct. It is reassuring to note that all six functionals uniformly predict a distinctly pyramidal coordination geometry about nitrogen.

From these results, we thus conclude that both of the 16e photoproducts studied react to form adducts containing anionic TEMPO ligands (refer back to Figure 1), effectively increasing the oxidation state of the metal centers by one. The bimolecular rate constants demonstrate that the reactions between these

Table 2. Experimental and Calculated Frequency Gap for the A_1 and B_1 Modes of $^2Fe(CO)_4(TEMPO)$

functional	$\Delta\upsilon$ [$A_1 - B_1$ modes] (cm^{-1})
B3LYP	54
BP86	65
M06	57
PBE0	55
PW91	67
WB97	54
experiment	56

16e species and TEMPO occur at or near the diffusion-limited rate.

3.2. Ultrafast Reactivity of TEMPO toward 17-Electron Radicals. In addition to the 16e photoproducts described thus far, we also explored the reactivity of the TEMPO radical toward odd-electron reaction intermediates. Photolysis of $[CpFe(CO)_2]_2$ and $Mn_2(CO)_{10}$ at 400 nm readily yields the corresponding 17e radicals, which serve as representative examples of 17e intermediates in organometallic reaction mechanisms. Note that we have elected to present spectra at higher TEMPO concentrations for these 17-electron photoproducts, so that formation of the corresponding TEMPO adduct could be readily observed on the ultrafast time scale.

3.2.1. Reactivity of TEMPO toward CpFe(CO)$_2$. In alkane solution, photolysis of $[CpFe(CO)_2]_2$ at 400 nm leads to formation of 17e $CpFe(CO)_2$ radicals, characterized by absorption bands at 1935 and 2006 cm^{-1} (the frequencies of which are shifted slightly in the data in 0.64 M TEMPO solution shown in Figure 5).[41] A CO-loss product, $Cp_2Fe_2(\mu$-$CO)_3$, is also formed and displays an absorption band at 1820 cm^{-1} (not shown);[41] this species did not show dynamic changes with delay time. Figure 5 shows TRIR spectra of $[CpFe(CO)_2]_2$ collected following 400 nm excitation in a 0.64 M solution of TEMPO in cyclohexane solvent. As the delay time increases, the bands at 1931 and 2003 cm^{-1}, corresponding to $CpFe(CO)_2$ (shifted slightly from those in neat cyclohexane), decay with the concomitant rise of new bands at 1972 and 2020 cm^{-1}, assigned to a $CpFe(CO)_2$(TEMPO) adduct. The fact that two bands are present in this adduct indicates that both CO ligands are still present. Note that the $CpFe(CO)_2$ band at 2003 cm^{-1} overlaps a parent bleach band at ~2005 cm^{-1}, which is not readily visible due to overlap with the more intense positive band. At a 0.64 M concentration of TEMPO, formation of the TEMPO adduct is not substantially complete within the experimentally accessible time delays, indicating that formation of the TEMPO adduct from $CpFe(CO)_2$ is notably slower than with either of the 16e photoproducts studied.[42] It does not appear that an equilibrium is reached on the time scale studied, as the peaks continue to show dynamic changes at delay times >1000 ps. In addition to the observed frequencies themselves, the fact that dynamic changes continue to occur beyond the first ~200 ps rules out the possibility of recombination of the nascent fragments to incorporate a bridging TEMPO ligand, as previous studies have demonstrated that picosecond bimolecular reactions involving the fragments cease after diffusion out of the solvent cage, which is complete within the first ~200 ps.

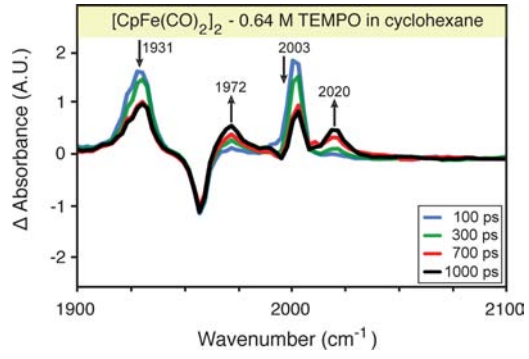

Figure 5. TRIR spectra of $[CpFe(CO)_2]_2$ in 0.64 M TEMPO/cyclohexane solution following 400 nm photolysis.

Noting that both the frequencies of the symmetric and antisymmetric CO-stretching modes of the $CpFe(CO)_2$ species increase upon coordination of the TEMPO ligand, it appears that the amount of electron density at the Fe center has decreased (i.e., that the metal center has been oxidized by coordination of TEMPO). For comparison, coordination of the strong 2e donor ligand $P(OMe)_3$ to $CpFe(CO)_2$ results in a decrease of the CO-stretching frequencies, indicative of an increase in π-backbonding to the CO-ligands. Thus, the experimental results in this case again point to an anionic TEMPO ligand. DFT calculations show a calculated pyramidal geometry at nitrogen for this adduct, using all six functionals tested (sum of angles equal to 336.5° with B3LYP), also indicating an anionic TEMPO ligand.

As shown in Table 3, DFT results with each of the hybrid functionals predict an increase in the CO-stretching frequencies of both modes upon coordination of TEMPO to $CpFe(CO)_2$, consistent with the experimental results. The pure DFT functionals tested (BP86 and PW91) instead predict similar frequencies for $CpFe(CO)_2$ and $CpFe(CO)_2$(TEMPO). Considering that the experimentally observed frequencies are clearly higher for the TEMPO adduct, consistent with the anionic ligand (whose geometry was correctly predicted by all of the functionals tested), this difference indicates that the pure DFT functionals do a poor job of describing the changes in vibrational frequencies for $CpFe(CO)_2$ upon coordination of a TEMPO ligand.

Table 3. Experimental and Calculated Frequency Shifts for CO-Stretching Modes upon Coordination of TEMPO (nitroxyl group) to $CpFe(CO)_2$

functional	$\Delta\upsilon_{symmetric}$ (cm^{-1})	$\Delta\upsilon_{antisymmetric}$ (cm^{-1})
B3LYP	40	22
BP86	6	−2
M06	40	21
PBE0	41	23
PW91	6	−3
WB97	59	37
experiment	41	17

3.2.2. Reactivity of TEMPO toward Mn(CO)$_5$. Photolysis of $Mn_2(CO)_{10}$ at 400 nm yields a pair of $Mn(CO)_5$ radicals, characterized by an absorption band at 1985 cm^{-1} in alkane solution.[43] Figure 6 shows TRIR spectra of $Mn_2(CO)_{10}$ collected following 400 nm excitation in a 0.64 M solution of TEMPO in cyclohexane. The bands at ~1985 cm^{-1} decrease with increasing delay time, along with the rise of bands at 2021−2033 (broad) and 2052 cm^{-1}, assigned to an $Mn(CO)_5$(TEMPO) adduct. The possibility of concomitant CO-loss (from $Mn(CO)_5$) to yield species with fewer CO ligands

dx.doi.org/10.1021/ja404476m | J. Am. Chem. Soc. 2013, 135, 11266−11273

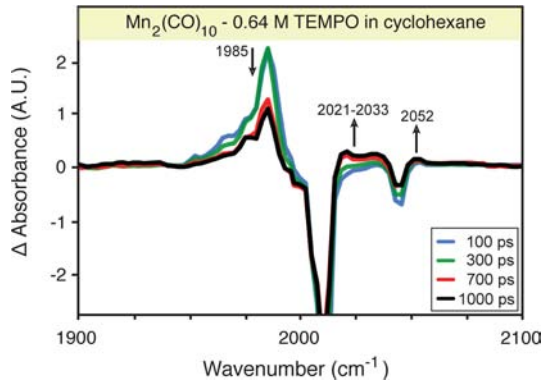

Figure 6. TRIR spectra of $Mn_2(CO)_{10}$ in 0.64 M TEMPO/cyclohexane solution following 400 nm photolysis.

was assessed via DFT frequency calculations, and these predicted a strong red-shift (~50−80 cm^{-1}) of the strongest CO-stretching absorption band, relative to bare $Mn(CO)_5$, in each case, thus ruling out potential CO-loss structures. Similar to the situation with $[CpFe(CO)_2]_2$, the fact that dynamic changes take place on time scales longer than that for diffusion out of the solvent cage eliminates the possibility of recombination to form an adduct with a bridging TEMPO ligand. Considering the delocalization of the vibrational modes of $Mn(CO)_5$, and lack of existing TRIR results on the coordination of ligands to $Mn(CO)_5$, it is not necessarily straightforward to correlate the experimentally observed frequency shifts to changes in the amount of electron density at the Mn center. DFT calculations were thus used to investigate the oxidation state of the metal center to check for consistency between the experimentally observed and calculated CO-stretching absorptions.

Similar to each of the other adducts in this study, all six functionals tested indicate that the $Mn(CO)_5(TEMPO)$ adduct adopts a pyramidal geometry about the nitrogen center (sum of angles = 333.8° using the B3LYP functional), again indicating an anionic TEMPO ligand. The calculated frequency shifts for $Mn(CO)_5(TEMPO)$, relative to bare $Mn(CO)_5$, are in good agreement with those observed experimentally; the highest intensity absorption band (observed experimentally at 1985 cm^{-1}) is predicted to remain at a similar frequency and decrease in intensity, with higher frequency bands becoming IR active at frequencies blue-shifted by ~20−85 cm^{-1} relative to the band at 1985 cm^{-1}. On the basis of comparison between the DFT results and the experimental spectra, we conclude that $Mn(CO)_5(TEMPO)$ is characterized by an anionic TEMPO ligand.

We point out that 17e complexes are typically fairly unreactive toward many 2e donor ligands, relative to their 16e counterparts, and that only strong Lewis bases (e.g., phosphines, phosphites) have been previously observed to undergo associative reaction mechanisms with 17e photoproducts on the ultrafast time scale.[44,45] Even among 17e photoproducts, $Mn(CO)_5$ is particularly unreactive in this regard, as a recent study demonstrated that it does not react to any detectable extent in concentrated $P(OMe)_3$ solutions on the picosecond time scale.[46] Also of relevance to the $Mn(CO)_5(TEMPO)$ adduct are previous studies that have isolated a final product of $Mn(CO)_3(TEMPO)$ from the reaction of TEMPO with $Mn_2(CO)_{10}$, with TEMPO behaving as an η^2 anionic ligand (refer back to Figure 1) in the 16e $Mn(CO)_3(TEMPO)$ complex.[16] This implies that to ultimately achieve the more thermodynamically stable product, $Mn(CO)_5(TEMPO)$ must loose two additional carbonyl ligands and rearrange its TEMPO ligand to an η^2 coordination geometry.

A final point we wish to make is that the fact the metal centers are clearly oxidized upon reaction with TEMPO (which is clear from the experimental data alone in the case of $CpCo(CO)$ and $CpFe(CO)_2$) is indication that the dynamic changes observed in the TRIR spectra cannot be the result of an electron transfer process independent of TEMPO coordination. Were this to be the case (i.e., were electron transfer to cause oxidation of the metal centers), electron transfer would need to occur from an already electron deficient metal center to TEMPO, and electron transfer *from* a species which is already electron deficient *to* a species which is stable under ambient conditions would be unprecedented. Were such a rare event to be observed, there is furthermore no reason it should take place with all four of the photoproducts studied. The time scales observed for this reaction at the concentrations studied are consistent with the body of existing literature surrounding bimolecular reactions involving electron deficient organometallic photoproducts on the picosecond time scale, and the DFT results further indicate both that TEMPO should coordinate to these metal centers as an anionic ligand, and that, upon coordination, the frequencies should shift in a manner consistent with the experimental observations.

4. CONCLUSIONS

In this study we have examined the reactivity of the TEMPO radical toward coordinatively unsaturated 16e and 17e metal carbonyl reaction intermediates. In each case, we observe that this coordinatively versatile ligand *coordinates to the metal center associatively with a concurrent internal oxidation−reduction process, yielding adducts with anionic TEMPO ligands*. The oxidation state of each metal center has thus increased by one, and these adducts are characterized by a pyramidal geometry at the nitroxyl nitrogen atom. Overall, the 16e complexes appear to react more readily with TEMPO than do the 17e complexes, despite the fact that TEMPO is a radical species. The fact that TEMPO coordinates to each of these intermediates similarly, as an anionic ligand, suggests that these results can be considered generally representative of the reactivity of TEMPO toward coordinatively unsaturated low-valent 16e and 17e reaction intermediates. In light of this result, one can rationalize the tendency for the TEMPO ligand to adopt an anionic character by the low-valency of the metal center, making the internal oxidation−reduction process facile.

This result is relevant to existing studies on TEMPO catalyzed reaction mechanisms. For example, Sheldon et al. have suggested a reaction mechanism in which TEMPO coordinates to a Cu(I) complex as an anionic ligand to yield a Cu(II) intermediate, which subsequently effects alcohol oxidation.[47] An alternative mechanism for this same reaction suggests a different role for the metal complex, where disproportionation of TEMPO yields a hydroxylamine which is then oxidized by the metal complex to yield the active catalytic speices, an oxoammonium TEMPO cation.[48] The latter mechanism has been proposed to characterize the same reaction catalyzed by a variety of other metals as well. While the present results do nothing to rule out the possibility of the latter mechanism, they clearly demonstrate that TEMPO can react as proposed in the former mechanism, via anionic

dx.doi.org/10.1021/ja404476m | J. Am. Chem. Soc. 2013, 135, 11266−11273

coordination to a low-valent metal center. Similar anionic coordination of TEMPO has also been proposed previously in other situations, such as a C−H arylation mechanism in which two TEMPO molecules coordinate as anionic ligands to a low-valent Rh(I) complex yielding a Rh(III) intermediate.[49] Other mechanisms have been proposed for reactions involving higher-valent metal complexes.

The structure and reactivity of organometallic TEMPO adducts are important to developing a clear understanding of their mechanistic role in a wide range of chemical processes, including the oxidation of alcohols, oxidative arene coupling, free radical polymerization, and radical trapping experiments. In addition to the insight gained into the chemistry of this important ligand, we have demonstrated that time-resolved infrared spectroscopy, combined with electronic structure calculations, allows for direct characterization of the structure of organometallic TEMPO adducts in the solution phase. Continued studies into the reactivity of well-characterized TEMPO complexes will help to further elucidate the mechanistic details and patterns governing TEMPO-mediated organometallic reactivity.

■ ASSOCIATED CONTENT

Supporting Information

DFT z-matrix coordinates for all structures listed in Tables 1, 2, and 3 and the full version of ref 32. This material is available free of charge via the Internet at http://pubs.acs.org.

■ AUTHOR INFORMATION

Corresponding Author

cbharris@berkeley.edu

Notes

The authors declare no competing financial interest.

■ ACKNOWLEDGMENTS

This work was supported by NSF Grant CHE-1213135. We acknowledge use of the Molecular Graphcis and Computation Facility at UC-Berkeley (Grants CHE-0840505, CHE-0233882). This research used resources of the National Energy Research Scientific Computing Center, which is supported by the Office of Science of the U.S. Department of Energy under Contract No. DE-AC02-05CH11231. S.C.N. acknowledges support through a VIED fellowship. J.P.L. acknowledges support through an NSF graduate research fellowship.

■ REFERENCES

(1) (a) Anelli, P. L.; Biffi, C.; Montanari, F.; Quici, S. *J. Org. Chem.* **1987**, *52*, 2559. (b) de Nooy, A. E. J.; Besemer, A. C.; van Bekkum, H. *Synthesis* **1996**, 1153. (c) De Souza, M. V. N. *Mini-Rev. Org. Chem.* **2006**, *3*, 155. (d) Vogler, T.; Studer, A. *Synthesis* **2008**, 1979. (e) Hoover, J. M.; Stahl, S. S. *J. Am. Chem. Soc.* **2011**, *133*, 16901.

(2) (a) Caron, S.; Dugger, R. W.; Ruggeri, S, G.; Ragan, J. A.; Ripin, D. H. B. *Chem. Rev.* **2006**, *106*, 2943. (b) Ciriminna, R.; Pagliaro, M. *Org. Process Res. Dev.* **2010**, *14*, 245.

(3) Lagunas, A.; Mairata i Payeras, A.; Jimeno, C.; Pericàs, M. A. *Org. Lett.* **2005**, *7*, 3033.

(4) Vogler, T.; Studer, A. *Org. Lett.* **2008**, *10*, 129.

(5) Maity, S.; Manna, S.; Rana, S.; Naveen, T.; Mallick, A.; Maiti, D. *J. Am. Chem. Soc.* **2013**, *135*, 3355.

(6) Lagunas, A.; Mairata i Payeras, A.; Jimeno, C.; Pericàs, M. A. *Chem. Commun.* **2006**, 1307.

(7) (a) Keana, J. F. W. *Chem. Rev.* **1978**, *78*, 37. (b) Volodarsky, L. B.; Reznikov, V. A.; Ovcharenko, V. I. *Synthetic Chemistry of Stable Nitroxides*; CRC Press: Boca Raton, FL, 1994. (c) Mak, K. W.; Yeung, S. K.; Chan, K. S. *Organometallics* **2002**, *21*, 2362. (d) Georges, M. K.; Veregin, R. P. N.; Kazmaier, P. M.; Hamer, G. K.; Saban, M. *Macromolecules* **1994**, *27*, 7228. (e) Connolly, T. J.; Baldoví, M. V.; Mohtat, N.; Scaiano, J. C. *Tetrahedron Lett.* **1996**, *28*, 4919. (f) Connolly, T. J.; Scaiano, J. C. *Tetrahedron Lett.* **1997**, *38*, 1133. (g) Patten, T. E.; Matyjaszewski, K. *Acc. Chem. Res.* **1999**, *32*, 895. (h) Knoop, C. A.; Studer, A. *J. Am. Chem. Soc.* **2003**, *125*, 16327. (i) Zetterlund, P. B.; Nakamura, T.; Okubo, M. *Macromolecules* **2007**, *40*, 8663.

(8) (a) Eaton, S. S.; Eaton, G. R. *Coord. Chem. Rev.* **1988**, *83*, 29. (b) Eaton, S. S.; Eaton, G. R. *Coord. Chem. Rev.* **1978**, *26*, 207. (c) Kelman, D. J.; Mason, R. P. *Arch. Biochem. Biophys.* **1993**, *306*, 439. (d) Smirnov, A. I.; Smirnova, T. I.; Morse, P. D., II. *Biophys. J.* **1995**, *68*, 2360. (e) Wróbel, A.; Jezierski, A.; Gomułkiewicz, J. *Free Rad. Res.* **1999**, *31*, 201. (f) Borisenko, G. G.; Martin, I.; Zhao, Q.; Amoscato, A. A.; Kagan, V. E. *J. Am. Chem. Soc.* **2004**, *126*, 9221.

(9) Forbes, G. C.; Kennedy, A. R.; Mulvey, R. E.; Rodger, P. J. A. *Chem. Commun.* **2001**, 1400.

(10) (a) Huang, K.-W.; Waymouth, R. M. *J. Am. Chem. Soc.* **2002**, *124*, 8200. (b) Huang, K.-W.; Han, J. H.; Cole, A. P.; Musgrave, C. B.; Waymouth, R. M. *J. Am. Chem. Soc.* **2005**, *127*, 3807.

(11) Jones, C.; Rose, R. P. *New J. Chem.* **2007**, *31*, 1484.

(12) Dickman, M. H.; Doedens, R. J. *Inorg. Chem.* **1982**, *21*, 682.

(13) (a) Dickman, M. H.; Doedens, R. J. *Inorg. Chem.* **1981**, *20*, 2677. (b) Laugier, J.; Latour, J.-M.; Canschi, A.; Rey, P. *Inorg. Chem.* **1991**, *30*, 4474.

(14) Scepaniak, J. J.; Wright, A. M.; Lewis, R. A.; Wu, G.; Hayton, T. W. *J. Am. Chem. Soc.* **2012**, *134*, 19350.

(15) (a) Jaitner, P.; Huber, W.; Gieren, A.; Betz, H. *J. Organomet. Chem.* **1986**, *311*, 379. (b) Jaitner, P.; Rieker, C.; Wurst, K. *Chem. Commun.* **1997**, 1245. (c) Jaitner, P.; Veciana, J.; Sporer, C.; Kopacka, H.; Wurst, K.; Ruiz-Molina, D. *Organometallics* **2001**, *20*, 568.

(16) Jaitner, P.; Huber, W.; Huttner, G.; Scheidsteger, O. *J. Organomet. Chem.* **1983**, *259*, C1.

(17) Jaitner, P.; Huber, W. *Inorg. Chim. Acta* **1987**, *129*, L45.

(18) (a) Bailey, W. F.; Bobbitt, J. M.; Wiberg, K. B. *J. Org. Chem.* **2007**, *72*, 4504. (b) Michel, C.; Belanzoni, P.; Gamez, P.; Reedijk, J.; Baerends, E. J. *Inorg. Chem.* **2009**, *48*, 11909. (c) Belanzoni, P.; Michel, C.; Baerends, E. J. *Inorg. Chem.* **2011**, *50*, 11896. (d) Qiu, J. C.; Pradhan, P. P.; Blanck, N. B.; Bobbitt, J. M.; Bailey, W. F. *Org. Lett.* **2012**, *14*, 350.

(19) Semmelhack, M. F.; Shmid, C. R.; Cortes, D. A.; Chou, C. S. *J. Am. Chem. Soc.* **1984**, *106*, 3374.

(20) Gamez, P.; Arends, I. W. C. E.; Reedijk, J.; Sheldon, R. A. *Chem Commun.* **2003**, 2414.

(21) Dijksman, A.; Arends, I. W. C. E.; Sheldon, R. A. *Org. Biomol. Chem.* **2003**, *1*, 3232.

(22) Sheldon, R. A.; Arends, I. W. C. E. *J. Mol. Catal. A: Chem.* **2006**, *251*, 200.

(23) Cheng, L.; Wang, J.; Wang, M.; Wu, Z. *Inorg. Chem.* **2010**, *49*, 9392.

(24) Hamm, P.; Kaindl, R. A.; Stenger, J. *Opt. Lett.* **2000**, *25*, 1798.

(25) *OriginPro*, version 8.0; OriginLab: Northampton, MA, 2007.

(26) (a) Becke, A. D. *J. Chem. Phys.* **1993**, *98*, 5648. (b) Perdew, J. P. *Phys. Rev. B* **1986**, *33*, 8822.

(27) Lee, C.; Yang, W.; Parr, R. G. *Phys. Rev. B* **1988**, *37*, 785.

(28) Zhao, Y.; Truhlar, D. G. *Theor. Chem. Acc.* **2008**, *120*, 215.

(29) (a) Perdew, J. P.; Burke, K.; Ernzerhof, M. *Phys. Rev. Lett.* **1996**, *77*, 3865. (b) Perdew, J. P.; Burke, K.; Ernzerhof, M. *Phys. Rev. Lett.* **1997**, *78*, 1396. (c) Adamo, C.; Barone, V. *J. Chem. Phys.* **1999**, *110*, 6158.

(30) The PW91 calculations used both PW91 exchange and correlation functionals. (a) Perdew, J. P.; Wang, Y. *Phys. Rev. B* **1992**, *45*, 13244. (b) Perdew, J. P.; Chevary, J. A.; Vosko, S. H.; Jackson, K. A.; Pederson, M. R.; Singh, D. J.; Fiolhais, C. *Phys. Rev. B* **1992**, 6671. (c) Perdew, J. P.; Chevary, J. A.; Vosko, S. H.; Jackson, K. A.; Pederson, M. R.; Singh, D. J.; Fiolhais, C. *Phys. Rev. B* **1993**, 4978.

(31) Chai, J.-D.; Head-Gordon, M. *J. Chem. Phys.* **2008**, *128*, 084106.

(32) Frisch, M. J. et al. *Gaussian09*, Revision B.01; Gaussian: Wallingford, CT, 2009.
(33) (a) McLean, A. D.; Chandler, G. S. *J. Chem. Phys.* **1980**, *72*, 5639. (b) Raghavachari, J. S.; Binkley, J. S.; Seeger, R.; Pople, J. A. *J. Chem. Phys.* **1980**, *72*, 650. (c) Wachters, A. J. H. *J. Chem. Phys.* **1970**, *52*, 1033. (d) Hay, P. J. *J. Chem. Phys.* **1977**, *66*, 4377.
(34) (a) Izgorodina, E. I.; Brittain, D. R. B.; Hodgson, J. L.; Krenske, E. H.; Lin, C. Y.; Namazian, M.; Coote, M. L. *J. Phys. Chem. A* **2007**, *111*, 10754. (b) Zhao, Y.; Truhlar, D. G. *J. Phys. Chem. A* **2008**, *112*, 1095. (c) Izgorodina, E. I.; Coote, M. L.; Radom, L. *J. Phys. Chem. A* **2005**, *109*, 7558. (d) Izgorodina, E. I.; Coote, M. L. *J. Phys. Chem. A* **2006**, *110*, 2486. (e) Izgorodina, E. I.; Coote, M. L. *Chem. Phys.* **2006**, *324*, 96.
(35) While the broad electronic absorption present at early times overlaps this band somewhat, the observed kinetics fit well to a single exponential decay.
(36) Bengali, A. A.; Bergman, R. G.; Moore, C. B. *J. Am. Chem. Soc.* **1995**, *117*, 3879.
(37) (a) Snee, P. T.; Payne, C. K.; Mebane, S. D.; Harris, C. B. *J. Am. Chem. Soc.* **2001**, *123*, 6909. (b) Lomont, J. P.; Nguyen, S. C.; Harris, C. B. *Organometallics* **2012**, *31*, 3947. (c) Lomont, J. P.; Nguyen, S. C.; Schlegel, J. P.; Zoerb, M. C.; Hill, A. D.; Harris, C. B. *J. Am. Chem. Soc.* **2012**, *134*, 3120. (d) Lomont, J. P.; Nguyen, S. C.; Zoerb, M. C.; Hill, A. D.; Schlegel, J. P.; Harris, C. B. *Organometallics* **2012**, *31*, 3582.
(38) O'Connor, J. M.; Casey, C. P. *Chem. Rev.* **1987**, *87*, 307.
(39) Carreoń-Macedo, J. L.; Harvey, J. N. *J. Am. Chem. Soc.* **2004**, *126*, 5789.
(40) Portius, P.; Yang, J.; Sun, X.-Z.; Grills, D. C.; Matousek, P.; Parker, A. W.; Towrie, M.; George, M. W. *J. Am. Chem. Soc.* **2004**, *126*, 10713.
(41) George, M. W.; Dougherty, T. P.; Heilweil, E. J. *J. Phys. Chem.* **1996**, *100*, 201.
(42) Our ability to collect spectra at higher concentrations was limited by the fact that TEMPO has a non-negligible absorption cross section at 400 nm and also tends to form a film on the calcium fluoride windows at high concentrations; thus, the quality of our TRIR spectra became poor at excessively high TEMPO concentrations.
(43) (a) Owrutsky, J. C.; Baronavski, A. P. *J. Chem. Phys.* **1996**, *105*, 9864. (b) Steinhurst, D. A.; Baronavski, A. P.; Owrutsky, J. C. *Chem. Phys. Lett.* **2002**, *361*, 513.
(44) (a) Kling, M. F.; Cahoon, J. F.; Glascoe, E. A.; Shanoski, J. E.; Harris, C. B. *J. Am. Chem. Soc.* **2004**, *126*, 11414. (b) Cahoon, J. F.; Kling, M. F.; Schmatz, S.; Harris, C. B. *J. Am. Chem. Soc.* **2005**, *127*, 12555.
(45) Yang, H.; Snee, P. T.; Kotz, K. T.; Payne, C. K.; Frei, H.; Harris, C. B. *J. Am. Chem. Soc.* **1999**, *121*, 9227.
(46) Lomont, J. P.; Nguyen, S. C.; Harris, C. B. *J. Phys. Chem. A* **2013**, *117*, 3777.
(47) (a) Sheldon, R. A.; Arends, I. W. C. E.; Ten Brink, G.-J.; Dijksman, A. *Acc. Chem. Res.* **2002**, *35*, 774. (b) Sheldon, R. A.; Arends, I. W. C. E. *Adv. Synth. Catal.* **2004**, *346*, 1051.
(48) (a) Ansari, I. A.; Gree, R. *Org. Lett.* **2002**, *4*, 1507. (b) Figiel, P. J.; Leskelä, M.; Repo, T. *Adv. Synth. Catal.* **2007**, *349*, 1173. (c) Salinas Uber, J.; Vogels, Y .; van den Helder, D.; Mutikainen, I.; Turpeinen, U.; Fu, W. T.; Roubeau, O.; Gamez, P.; Reedijk, J. *Eur. J. Inorg. Chem.* **2007**, 4197. (d) Mannam, S.; Alamsetti, S. K.; Sekar, G. *Adv. Synth. Catal.* **2007**, *349*, 2253. (e) Lu, N.; Lin, Y.-C. *Tetrahedron Lett.* **2007**, *48*, 8823. (f) Jiang, N.; Ragauskas, A. J. *J. Org. Chem.* **2006**, *71*, 7087. (g) Gamez, P.; Arends, I. W. C. E.; Sheldon, R. A.; Reedijk, J. *Adv. Synth. Catal.* **2004**, *346*, 805. (i) Striegler, S. *Tetrahedron* **2006**, *62*, 9109. (h) Velusamy, S.; Srinivasan, A.; Punniyamurthy, T. *Tetrahedron Lett.* **2006**, *47*, 923. (j) Ragagnin, G.; Betzemeier, B.; Quici, S.; Knochel, P. *Tetrahedron* **2002**, *58*, 3985. (k) Semmelhack, M. F.; Schmid, C. R.; Cortés, D. A.; Chou, C. S. *J. Am. Chem. Soc.* **1984**, *106*, 3374.
(49) Vogler, T.; Studer, A. *Org. Lett.* **2008**, *10*, 129.